Protective effects of *PI3KCG* gene on acute myocardial infarction

Ge Gong[1,2]*, Xin-Xing Yang[1]*, Yan-Yan Li[1], Hong-Yu Geng[1], Hui Wang[3], Lian-Sheng Wang[3], Zhi-Jian Yang[3]

[1]Departments of Geriatrics, the First Affiliated Hospital of Nanjing Medical University, Nanjing 210029, China; [2]Departments of Geriatrics, General Hospital of Nanjing Military Region, Nanjing 210002, China; [3]Departments of Cardiology, the First Affiliated Hospital of Nanjing Medical University, Nanjing 210029, China

Contributions: (I) Conception and design: YY Li; (II) Administrative support: H Wang, LS Wang, ZJ Yang; (III) Provision of study materials or patients: YY Li; (IV) Collection and assembly of data: G Gong, HY Geng, YY Li, LS Wang; (V) Data analysis and interpretation: G Gong, XX Yang, YY Li; (VI) Manuscript writing: All authors; (VII) Final approval of manuscript: All authors.

*These authors contributed equally to this work.

Correspondence to: Dr. Yan-Yan Li. Department of Geriatrics, First Affiliated Hospital of Nanjing Medical University, Nanjing 086-210029, China. Email: lyynjmu123@126.com.

Background: To study the protective effects of recombinant phosphatidylinositol 3-kinase p110 gamma (*rPLV-PI3KCG*) lentiviral vector in Sprague-Dawley (SD) rats with acute myocardial infarction (AMI).

Method: The AMI rat models were established by ligaturing left anterior descending coronary artery. The *rPLV-PI3KCG* or empty lentiviral vectors were injected at the edge of the infarct zone. The experiment was divided randomly into four groups (n=8): (I) Sham group; (II) AMI group; (III) AMI + empty vector injection group (AMI + E group); and (IV) AMI + PLV-PI3KCG injection group (AMI + PLV-PI3KCG group). The ultrasonic cardiogram (UCG) was used to compare the structural or functional changes among the four groups after operation for 10 days. Meanwhile, the rats were sacrificed and HE staining was used to compare the myocardial tissue changes among the four groups. The immunofluorescence and western blots were performed to compare the angiogenesis in the infarct region and explore the mechanism of the protective effects of *PI3KCG* gene on AMI rats.

Results: Compared with AMI group and AMI + E group, in the AMI + PLV-PI3KCG group, left ventricular end diastolic diameter (LVEDd) was decreased, left ventricular ejection fraction (LVEF%) was significantly increased, and vascular endothelial growth factor (VEGF) expression was significantly increased in the infarct region (P<0.05); PI3KCG, pAkt/Akt, HIF-1a, and Bcl-2/Bax protein expressions were significantly increased (P<0.05).

Conclusions: The *rPLV-PI3KCG* injection could improve the cardiac function, relieve the cardiac injury after the AMI operation. *PI3KCG* gene could play the protection role in the AMI process possibly by activating PI3K/Akt signal pathway, inhibiting apoptosis and promoting angiogenesis.

Keywords: *PI3KCG*; apoptosis; acute myocardial infarction (AMI); lentiviral vector

Introduction

Myocardial apoptosis was involved in the pathogenesis of acute myocardial infarction (AMI). The recombinant phosphatidylinositol 3-kinase p110 gamma (PI3KCG) lentiviral vector plasmid (*rPLV-PI3KCG*) was constructed through the method of homologous recombination, and the *rPLV-PI3KCG* vector was transfected into primary neonatal rat cardiomyocytes. The result showed that *PI3KCG* gene could protect against the hypoxia reoxygenation cardiomyocytes injury at the cellular level (1). It was speculated that this protective mechanism might

be associated with PI3K/Akt signaling pathway activation and apoptosis inhibition. PI3K has I, II, III three subtypes; PI3K I type is a dimeric enzyme that consists of a regulatory subunit and a catalytic subunit, wherein the catalytic subunit is divided into class IA (p110α, p110β and p110δ) and class IB (p110γ) (2). PI3K/Akt signal pathway widely existed in various tissues which play an important role in the cellular growth, differentiation, metabolism, survival, and proliferation process. When type 1 PI3K interacted with the cell surface receptor, as the receptors of growth factor, insulin, it could be activated by changing the conformation and then phosphorylate the substrate 3,4-diphosphoinositide (PIP2) and transform it to 3,4,5-triphosphoinositide (PIP3). The downstream effector molecule of PI3K is Akt, the 57 kDa serine/threonine protein kinase. Akt could promote the cellular growth and suppress apoptosis by phosphorylating various cellular proteins, as kinase and tumor inhibition factor.

In 2010, Lin *et al.* found that activation of PI3K (p110 alpha) protects the heart against myocardial infarction (MI)-induced heart failure. It was indicated that PI3K (p110 alpha) is important for maintaining cardiac function in a setting of MI and that elevated levels of PI3K are beneficial. They concluded that cardiac-selective targets that mediate the protective effects of PI3K represent new drug targets for heart failure (3). In 2016, Liu *et al.* found that dihydromyricetin pretreatment provided significant protection against ischemia reperfusion (I/R)-induced myocardial injury, including enhanced antioxidant capacity and inhibited apoptosis in vivo and in vitro. This protection effect correlated with the activation of the PI3K/Akt and HIF-1α signaling pathways (4). In 2016, Yang *et al.* found that tumor necrosis factor (TNF)-like weak inducer of apoptosis (TWEAK), protected the cardiac apoptosis by activation of cardioprotective signaling PI3K/Akt during I/R. Their findings suggest that TWEAK may represent a cardioprotective factor that inhibits the myocyte death of myocardial IR injury in a PI3K/Akt pathway dependent manner (5).

In 2017, Su *et al.* found that nicorandil pretreatment reduced hypoxia-induced cardiomyocyte apoptosis and improved cardiomyocyte-survival rate through PI3K/Akt signaling pathway in coronary microembolization in rats (6). Li *et al.* also found that overexpression of corin protected cardiomyocytes from H_2O_2-induced injury by decreasing apoptosis via activations of the PI3K/Akt signaling pathway (7).

As we have verified the protective effect of *PI3KCG* gene at the cardiomyocyte level through the anti-apoptotic mechanism on the early stage (1), in order to verify the protective effect of *PI3KCG* gene at the integral level through its anti-apoptotic and angiogenesis mechanisms, we established the AMI rat model, injected the *rPLV-PI3KCG* vector into the AMI heart and observed the *PI3KCG* gene protection effect on the AMI rat model.

Methods

Experimental animals, reagents and instrument

The Sprague-Dawley (SD) rats were provided by Experimental Animal Center of our University and each rat weighed 200–220 g. *rPLV-PI3KCG* lentiviral vector were constructed by homologous recombination method and purified in our lab with the concentration 1×10^8 IU/mL (1).

PI3K mouse-anti-rat polyclonal antibody (Abcam, Cambridge, UK), TGF-β1 rabbit anti-rat polyclonal antibody (Cell Signaling, Danvers, MA, USA), Bax rabbit anti-rat polyclonal antibody (Cell Signaling), Bcl-2 rabbit anti-rat monoclonal antibody (Cell Signaling), GAPDH rabbit anti-rat monoclonal antibody (Cell Signaling), phospho-Akt (ser473) (pAkt) rabbit anti-rat antibody (Cell Signaling), Akt rabbit anti-rat antibody (Cell Signaling), Caspase 3 rabbit anti-rat antibody (Cell Signaling), Hypoxia inducible factor (HIF-1α) (D2U3T) rabbit anti-rat antibody (Cell Signaling), vascular endothelial growth factor (VEGF) rabbit antibody (BioVision, San Francisco, USA), HRP-conjugated goat anti-rabbit secondary antibody (Santa Cruz, USA), HRP-conjugated goat anti-mouse secondary antibody (Santa Cruz, USA), Donkey F(ab)2 Anti-Rabbit IgG H&L (Alexa Fluor® 568) preadsorbed (Abcam, Cambridge, UK).

High-resolution small animal ultrasound system (VisualSonics, Toronto, Canada), the ultrasound probe (RMV716), small animal ventilator (ALC-V8S, Shanghai Alcott Biotech Co., Ltd., Shanghai, China), Micro-syringe (MC100ul, Shanghai Guangzheng medical instruments company, Shanghai, China), Freezing microtome (CM 1950, Leica Biosystems, Nussloch, German).

Establishment of AMI rats model by coronary ligation (8)

Our current research was approved by the Ethics Committee of our institute. Rats were anesthetized by the intraperitoneal (IP) injection of 10% chloral hydrate (0.3 mL/100 g) and then placed in a supine position. After

endotracheal intubation, artificial mechanical ventilation was used with a tidal volume of 2–3 mL, an inspiratory and expiratory ration of 1:1.5, and a respiratory rate of 75 breaths per min. After a left thoracotomy incision 1.5 cm from the third to fourth ribs, the pericardium was cut and the heart, exposed. The left coronary vein at the junction of pulmonary cone and left atrial appendage were taken as a symbol. A 6-0 nylon suture was placed at the edge of the left auricle about 0.15 cm around left ventricular branch. The color of the infarcted zone changed from red to white. In the Sham group, the suture was threaded through the same part of the heart, but not ligated. For the AMI + PLV-PI3KCG group, the *rPLV-PI3KCG* was injected at the edge of infarction region. After the operation, the chest cavities were sutured closed and the rats were fed for 10 days in a normal manner.

The 20 µL *rPLV-PI3KCG* or empty lentiviral vector at a concentration of 1×10^8 IU/mL was injected using micro-injection syringes. The rats were randomly divided into four groups (n=8): (I) sham-operated group (Sham group); (II) AMI group; (III) AMI + empty vector injection group (AMI + E group); and (IV) AMI + *rPLV-PI3KCG* injection group (AMI + PLV-PI3KCG group). Six to eight rats were included in each group for one trial. Eight trials were involved in the experiment (*Figure S1*).

Cardiac structure or function detection by ultrasonic cardiogram (UCG) (9)

Our current research was approved by the Ethics Committee of our institute. Ten days after the AMI surgery, heart function of each group was tested by a high-resolution small animal ultrasound system. The frequency of the ultrasonic probe was 20–23.5 MHz. After anesthesia [IP injection of 10% chloral hydrate (0.3 mL/100g)] rats were moved to a fixed supine position and chest skin prepared. Ventricular wall motion was observed by taking left ventricular long-axis and left ventricular papillary muscle short-axis of the sternum left margin. After measuring the interventricular septal thickness at diastole (IVSd), left ventricular end diastolic diameter (LVEDd), and left ventricular posterior wall diastolic diameter (LVPWd) using two-dimensional image-guided M-mode, left ventricular ejection fraction (LVEF%) and fractional shortening (FS%) were calculated. Each index was measured for three cardiac cycles. The average of these values was calculated and used in our analysis.

Hematoxylin and eosin (H&E) staining for the cardiac frozen sections

After UCG, the rat hearts were removed immediately after euthanasia, and coated with optimal cutting temperature (OCT) embedding medium and put into liquid nitrogen. The frozen hearts were cut into frozen sections of 6 µm in thickness by using the frozen section cut machine. Each section contained both left and right ventricles and ventricular septa and was stored at –80 ℃.

Frozen sections from the four groups were removed from the freezer, fixed with 4% paraformaldehyde for 10 min, and then washed 3–4 times with tap water before being immersed in filtered Harris Hematoxylin. After 2 minutes, sections were washed with warm tap water until the nuclei turn blue. The sections were then rinsed several dips in acid alcohol (0.5% HCL in 70% ethanol) and immersed in tap water for 5 min. The cytoplasm was stained by dipping slides several times in eosin. After removing excess eosin, slides were dehydrated with ethanol (from 95–100% ethanol), cleared with xylenes, and then mounted with a xylene-based mounting medium. Stained sections were observed under electron microscope and photographed.

Immunofluorescent staining for the cardiac frozen sections

After removing sections from the freezer, Tm was allowed to rest at RT for 30 minutes. The sections were then rinsed with phosphate buffer saline (PBS) and fixed in 100% acetone for 10 min at 4 ℃. After rinsing sections in PBS, the sections were circled with a pap pen and blocked with normal lamb serum (3% in PBS) for 45 minutes. The normal serum was then removed without washing, and the sections incubated with VEGF or Caspase 3 rabbit anti-rat polyclonal antibody at a 1:100 dilution at 4 ℃ overnight. Afterwards, the sections were rinsed with PBS and then incubated for 1 h with a 1:1,000 dilution of donkey F(ab)2 anti-rabbit IgG H&L (Alexa Fluor® 568) secondary antibody at room temperature in a dark humidified box. After washing sections with PBS, 4',6-diamidino-2-phenylindole (DAPI) was added to the sections for 5 minutes, and then the sections were washed with PBS. After mounting sections with AntiFade Fluorescence Mounting Medium and covering the slide with a cover glass, the sections were observed under fluorescent microscope and photographed.

Measuring protein expression of cardiac tissue by Western blot

After the cardiac ultrasonic detection, the rat hearts were taken out immediately and stored at –80 ℃. Cardiac tissues were lysed with radioimmunoprecipitation assay (RIPA) lysis buffer to extract the total protein. Thirty-six μg total protein was used for each Western blot trial after protein quantification. The proteins were separated by electrophoresis on 10% sodium dodecyl sulfate polyacrylamide gel electrophoresis (SDS-PAGE) and then transferred to polyvinylidene fluoride (PVDF) membranes. After being blocked with 5% skim milk at room temperature for 2 hours, the membranes were incubated with primary antibodies against PI3KCG, pAkt, Akt, Bax, Bcl-2, HIF-1α, and GAPDH overnight at 4 ℃ (all of the primary antibodies were used as 1:1,000 dilution concentration). Then they were added to the corresponding HRP-labeled secondary antibody (1:5,000) and incubated for 2 hours at 4 ℃. The blots were developed and photographed.

Statistical method

SPSS 20.0 statistical software was used to analyze the data. Measurement data were used as mean ± standard deviation in the name of ($\bar{x} \pm s$). A *t*-test was used to compare the measurement data between two groups; one-way ANOVA method was used to compare the measurement data among multiple groups. The significant difference level was set at P<0.05 level.

Results

The optimal rPLV-PI3KCG vector injection concentration determination

According to the different titers of rPLV-PI3KCG lentiviral vector injected, the SD rats were randomly divided into 2.5×10^6, 5×10^6, 1×10^7, 2.5×10^7, 5×10^7, and 1×10^8 IU/mL group. Compared with AMI group, AMI + E group and other different titer groups in the 1×10^8 IU/mL group, the LVEF% and FS% were significantly increased (P<0.05), LVEDd was significantly decreased (P<0.05). Compared with Sham group, in the AMI group, AMI + E group and other different titer groups, the LVEF%, FS% were significantly decreased (P<0.05), LVEDd was significantly increased (P<0.05) (*Figure S2*). Hence, it was indicated that the 1×10^8 IU/mL injection concentration had the optimal protective effects in the AMI process. The AMI + PLV-

PI3KCG group rats were injected with 20 μL of rPLV-PI3KCG vector in accordance with 1×10^8 IU/mL titer in the following experiments.

### *Cardiac structure or function changes detected by UCG*

For 10 days after the AMI operation, M-mode echocardiography showed normal results in the Sham group. The heart displayed coordinated and strong contraction and the thickness of each wall in the rat heart was normal. The electrocardiogram (ECG) had normal QRS wave. In the AMI group and AMI + E group, the wall motion weakened, disappeared, or even reversed. The left ventricular wall underwent a ball-like expansion and the ECG showed abnormal QRS waves and a variety of arrhythmias. In AMI + PLV-PI3KCG group, however, showed relatively little signs of damage. The wall motion was coordinated, contraction remained strong, and the left ventricular cavity size was normal. The ECG still had normal QRS wave (*Figure 1A*).

Compared with the Sham group, the AMI group and AMI + E groups had increased LVEDd and decreased LVEF% and FS% values (LVEDd—Sham group: 6.28±0.87 mm, AMI group: 7.65±0.77 mm, AMI + E group: 7.61±0.59 mm, P<0.05; LVEF%—Sham group: 83.87%±7.28%, AMI group: 50.26%±6.72%, AMI + E group: 49.47%±2.46%, P<0.05; FS%—Sham group: 44.03%±9.17%, AMI group: 18.58%±7.59%, AMI + E group: 18.49%±3.06%, P<0.05). After injection of the rPLV-PI3KCG, the LVEDd significantly decreased (6.50±0.55 mm, P<0.05) while the LVEF% and FS% value improved significantly (69.95%±2.51%, 35.66%±2.12%, respectively, P<0.05). In short, while left ventricular systolic function was significantly decreased in the AMI and AMI + E groups, it improved after the rPLV-PI3KCG injection. In addition, the cardiac size expansion in the AMI or AMI + E group was also inhibited after the heart was injected with rPLV-PI3KCG. There were no significant statistical differences in IVD and LVPWd between the different groups (P>0.05) (*Figure 1B,C*).

The cardiac pathological changes by H&E staining

The Sham group showed a normal structure with an even distribution pink myocardial cells and short, interconnected columnar cells forming a network. Each myocardial cell had an oval nucleus of uniform size was located its center. Myocardial tissue collected from the AMI group and
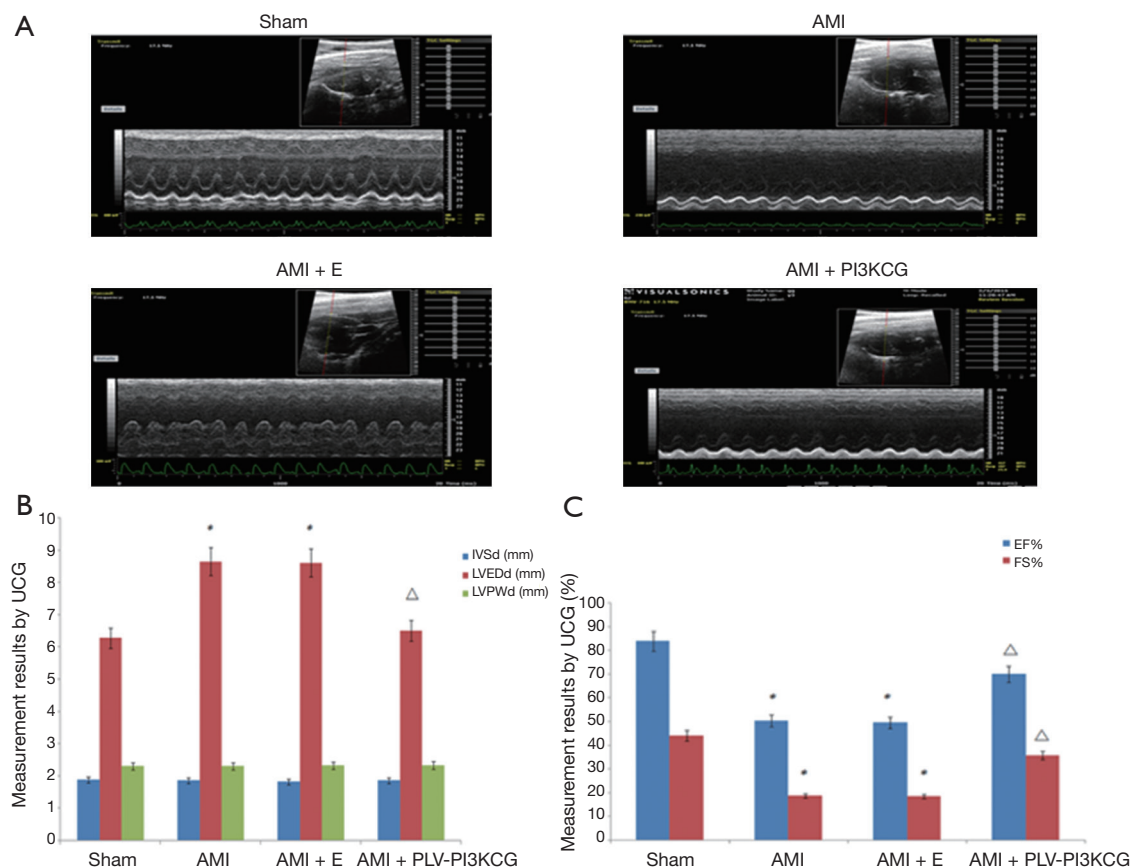
Figure 1 The cardiac M-mode ultrasonic images changes among the four experimental groups. (A) In sham group, each cardiac wall thickness was normal, the heart movement was coordinated and strong, and in ECG, QRS wave was normal. But in AMI group and AMI + E group, the cardiac wall motion was weakened or disappeared, some were reverse movement, the left ventricular cavity was ball-like expansion, and the ECG had the abnormal QRS wave, showing the different types of arrhythmias. However, in AMI + PLV-PI3KCG group, the wall motion was coordinated, the contraction was strong, the left ventricular cavity size was normal, and the ECG still had normal QRS wave. (B) The IVSd, LVEDd and LVPWd changes results detected by UCG. Compared with Sham group, in AMI group and AMI + E group, the LVEDd was significantly increased (P<0.05). After injection of *rPLV-PI3KCG* vector at myocardial infarct border zone, the LVEDd was significantly decreased (P<0.05). There were no significant statistical differences in IVDs and LVPWd between the different groups (P>0.05). (C) The LVEF% (EF%) and FS% changes results detected by UCG. Compared with Sham group, in AMI group and AMI + E group, the LVEF% and FS% values were decreased significantly (P<0.05). After injection of *rPLV-PI3KCG* vector at myocardial infarct border zone, the LVEF% and FS% values were significantly improved than before (P<0.05). *, compared with AMI group, AMI + E group, P<0.05; ᐃ, compared with Sham group, P<0.05. ECG, electrocardiogram; AMI, acute myocardial infarction; IVSd, interventricular septal thickness at diastole; LVEDd, left ventricular end diastolic diameter; LVPWd, left ventricular posterior wall diastolic diameter; LVEF%, left ventricular ejection fraction.

AMI + E group, on the other hand, were disordered and damaged. The tissue showed infiltration by large numbers of inflammatory cells. Compared with tissues collected from the AMI group and AMI + E group, tissues from AMI + PLV-PI3KCG group exhibited less infiltration by inflammatory cells and showed better organization. The

infarct size was also measured using the color pathological image analysis system (10). The infarcted size in the AMI and AMI + E groups is 50.12%±2.57% and 51.29%±2.60%, respectively. While in the AMI + PLV-PI3KCG group, the infarcted size was 26.34%±1.28% which was significantly lower than that in AMI and AMI + E groups (P<0.05) (*Figure 2*).
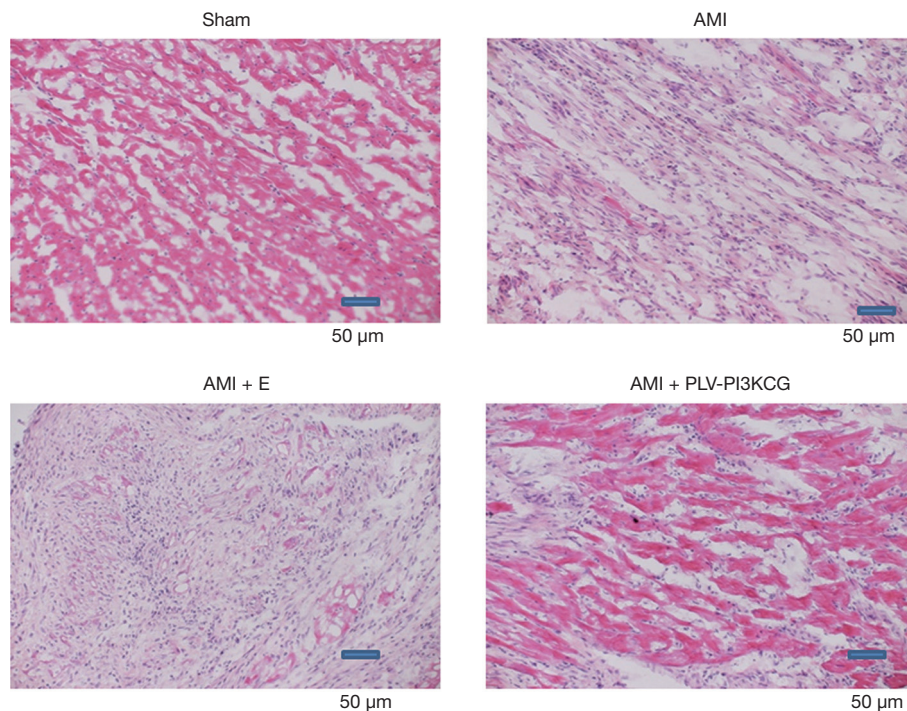
Figure 2 The cardiac pathological changes by H&E staining with electron microscopy (×200). In Sham group, it was showed that the evenly pink myocardial cells, with normal and clear structure, were short columnar and interconnected to form a network. Oval nuclear with uniform size was located in the center of myocardial cell. In AMI group, myocardial tissues were disordered and damaged, and a large number of inflammatory cells were infiltrated. In AMI + E group, myocardial tissues were disordered and damaged, and a large number of inflammatory cells were infiltrated. In AMI + PLV-PI3KCG group, compared with AMI group and AMI + E group, it was showed that myocardial tissue with less inflammatory cells infiltration was arranged relatively neatly. AMI, acute myocardial infarction.

### Changes of cardiac VEGF or Caspase 3 expression by immunofluorescent staining method

VEGF was primarily expressed in vascular endothelial cells in the myocardial tissue. Positive signaling was dependent on the successful merging of the red and blue fluorescence, indicating positive VEGF expression and the cell nucleus, respectively. Failure to merge indicated a false positive. Compared with Sham group, the relative level of VEGF fluorescence intensity in AMI group and AMI + E group was much lower in the MI region (Sham group: 1.00, AMI group: 0.39±0.021, AMI + E group: 0.41±0.031 P<0.05). Treatment with PLV-PI3KCG increased VEGF expression (0.76±0.035, P<0.05), suggesting the *PI3KCG* gene could promote angiogenesis in MI region (*Figure 3A,B*).

Cleaved Caspase 3 was primarily expressed in cardiomyocytes nucleus which is the activated form of Caspase 3. Compared with Sham group, the relative level of cleaved Caspase 3 fluorescence intensity in AMI group

and AMI + E group was much higher in the MI region (Sham group: 1.00, AMI group: 1.61±0.041, AMI + E group: 1.63±0.042 P<0.05). Treatment with PLV-PI3KCG decreased cleaved Caspase 3 expression (1.21±0.032, P<0.05), suggesting the *PI3KCG* gene could inhibit apoptosis in MI region (*Figure 4A,B*).

Protein expression in the AMI process as detected by Western blot

Compared to the Sham group, the AMI and AMI + E group expressed lower levels of PI3KCG, pAkt/Akt, and Bcl-2 and higher levels of Bax. Injection of *rPLV-PI3KCG* had the direct opposite effect. Compared to the AMI and AMI + E group, the AMI + PLV-PI3KCG group showed increased levels of PI3KCG, pAkt/Akt, and Bcl-2 and decreased levels of Bax expression. This supports the idea of the *PI3KCG* gene playing an important role in the AMI injury process by
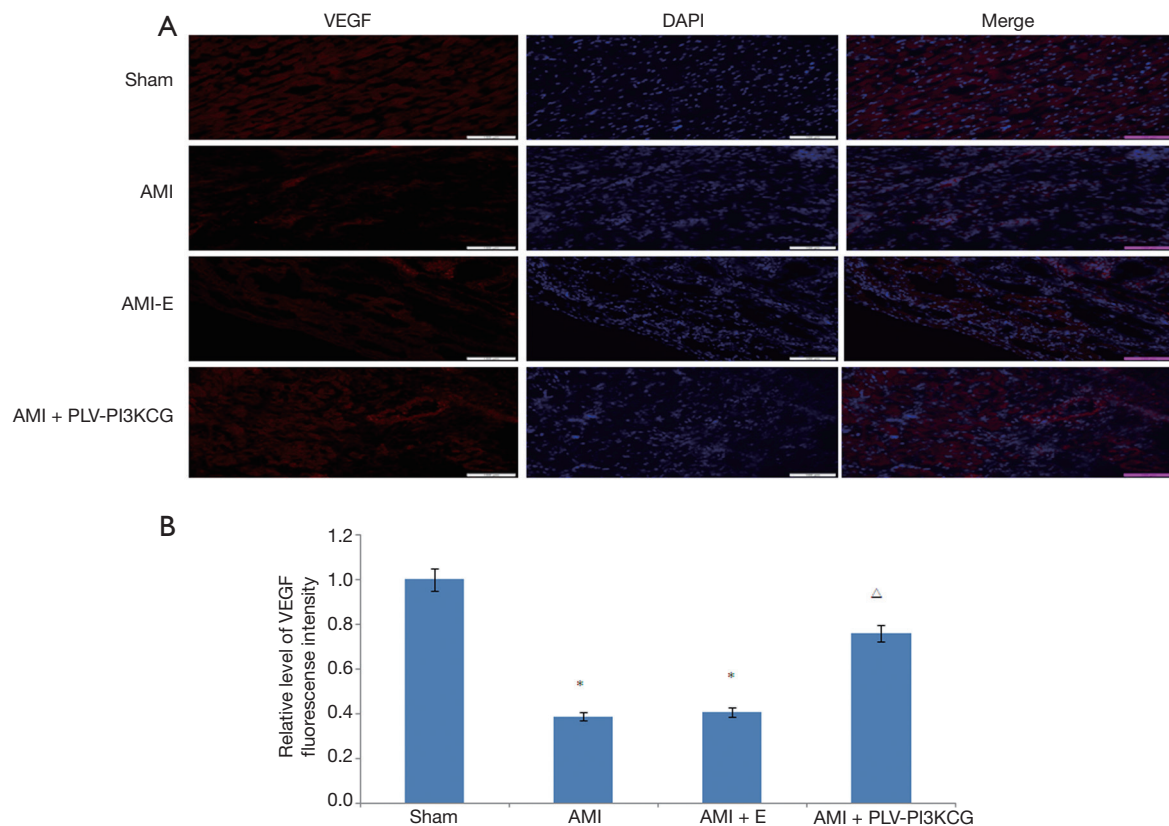
Figure 3 Comparation of VEGF expression in the infarction area among the four groups by immunofluorescence with laser microscope (×200). (A) VEGF was mainly expressed in vascular endothelial cells of myocardial tissue, with the positive expression site stained red and cell nucleus stained blue. (B) The relative level of VEGF fluorescence intensity in the AMI process. Compared with Sham group, VEGF expressions in AMI group and AMI + E group were significantly decreased in the myocardial infarction region (P<0.05). Compared with AMI group and AMI + E group, VEGF expression in AMI + PLV-PI3KCG group were significantly increased (P<0.05). *, compared with AMI group, AMI + E group, P<0.05; △, compared with Sham group, P<0.05. The scale in each picture means 100 μm. VEGF, vascular endothelial growth factor; AMI, acute myocardial infarction.

inhibiting apoptosis (*Figure 5A*).

Compared with Sham group, the AMI group and AMI + E group had significantly lower PI3KCG/GAPDH ratios (Sham group: 0.46±0.03, AMI group: 0.16±0.06, AMI + E group: 0.17±0.05, P<0.05). Compared with AMI group and AMI + E group, the AMI + PLV-PI3KCG group had significantly higher PI3KCG/GAPDH (0.38±0.07, respectively, P<0.05) (*Figure 5B*).

Compared to the Sham group, the AMI group and AMI + E groups had a significantly lower Bcl-2/Bax ratio (Sham group: 1.77±0.07, AMI group: 0.14±0.008, AMI + E group: 0.27±0.007, P<0.05). Compared with AMI group and AMI + E group, the AMI + PLV-PI3KCG group had a significantly higher Bcl-2/Bax ratio (1.64±0.09, P<0.05) (11) (*Figure 5C*).

Compared to the Sham group, the AMI group and AMI + E groups had a significantly lower pAkt/Akt ratio (Sham group: 0.64±0.04, AMI group: 0.21±0.008, AMI + E group: 0.26±0.007, P<0.05). Compared with AMI group and AMI + E group, the AMI + PLV-PI3KCG group had a significantly higher pAkt/Akt ratio (0.82±0.05, P<0.05) (*Figure 6A,B*).

As *Figure 7* shows, compared with Sham group, the HIF-1α protein in AMI group and AMI + E group expression was not significantly altered. Compared with AMI group and AMI + E group, the HIF-1α protein in AMI + PLV-PI3KCG group was significantly increased (*Figure 7A*). Regarding to HIF-1α/GAPDH protein expression ratio, there was no significant difference between the Sham group, AMI group or AMI + E group (Sham group: 0.94±0.08,
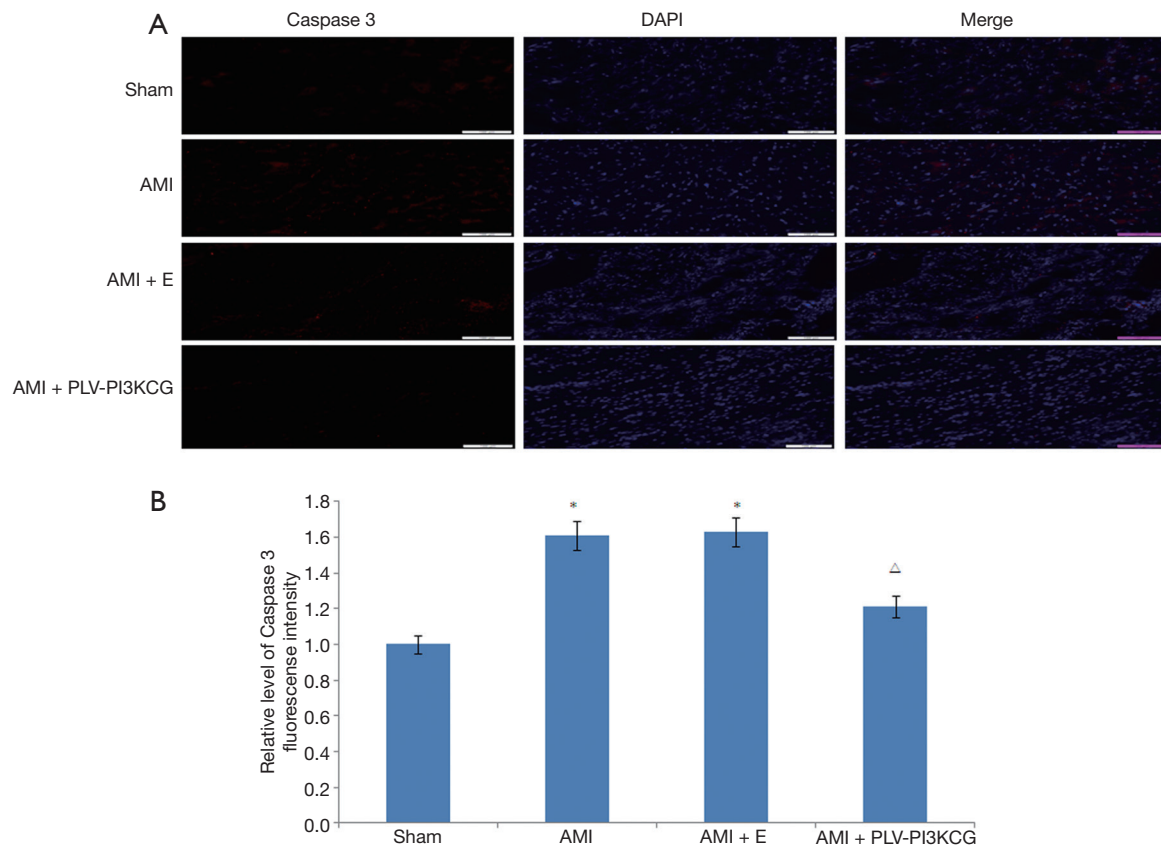
Figure 4 Comparation of cleaved Caspase 3 expression in the infarction area among the four groups by immunofluorescence with laser microscope (×200). (A) cleaved Caspase 3 was mainly expressed in nucleus of cardiomyocytes, with the positive expression site stained red and cell nucleus stained blue. (B) The relative level of cleaved Caspase 3 fluorescence intensity in the AMI process. Compared with sham group, cleaved Caspase 3 expressions in AMI group and AMI + E group were significantly increased in the myocardial infarction region (P<0.05). Compared with AMI group and AMI + E group, cleaved Caspase 3 expression in AMI + PLV-PI3KCG group were significantly decreased (P<0.05). *, compared with AMI group, AMI + E group, P<0.05; △, compared with Sham group, P<0.05. The scale in each picture means 100 μm. AMI, acute myocardial infarction.

AMI group: 0.93±0.07, AMI + E group: 0.95±0.09, P>0.05). However, HIF-1α in the AMI + PLV-PI3KCG group had a significantly higher level than other three groups (1.67±0.11, P<0.05) (*Figure 7B*).

Discussion

In this study, it was shown that $1×10^8$ IU/mL titer was the optimal concentration for the protective effect of *rPLV-PI3KCG* lentiviral vector. By comparison with Sham group, in the AMI group and AMI + E group, the heart function was significantly decreased, MI region was deranged, fiber was broken, and a large number of inflammatory cells were infiltrated. Besides, VEGF expression decreased,

cleaved Caspase 3 expression increased, PI3KCG protein expressions also decreased, pAkt/Akt and Bcl-2/Bax ratio decreased. These results illustrated that the AMI rat model was successfully established. At the stage of myocardial ischemia, inflammatory cell infiltration and decreased production of vascular endothelial cells inhibited PI3K/Akt signaling pathway, because decreased PI3K and pAkt expressions blocked activation of receptor regulatory proteins Smad2 (12), activating the expression of apoptotic gene Bax, cleaved Caspase 3 and inhibiting the expression of anti-apoptotic gene Bcl-2.

There was no significant difference between AMI group and AMI + E group, indicating that injection of lentivirus had no significant effect on this test. Compared
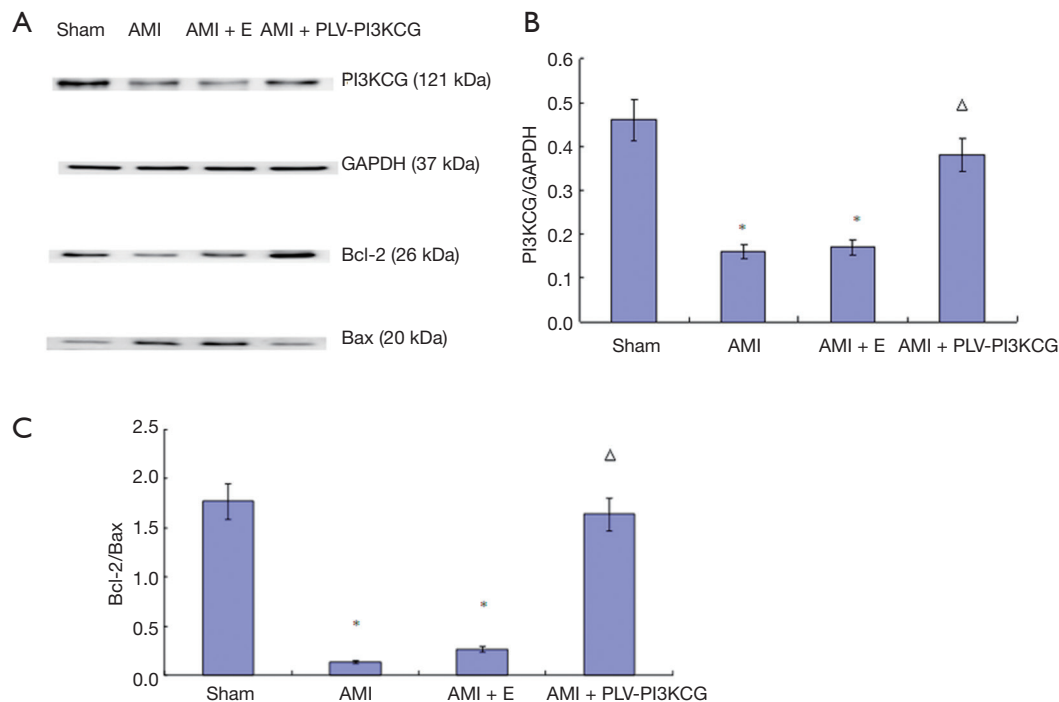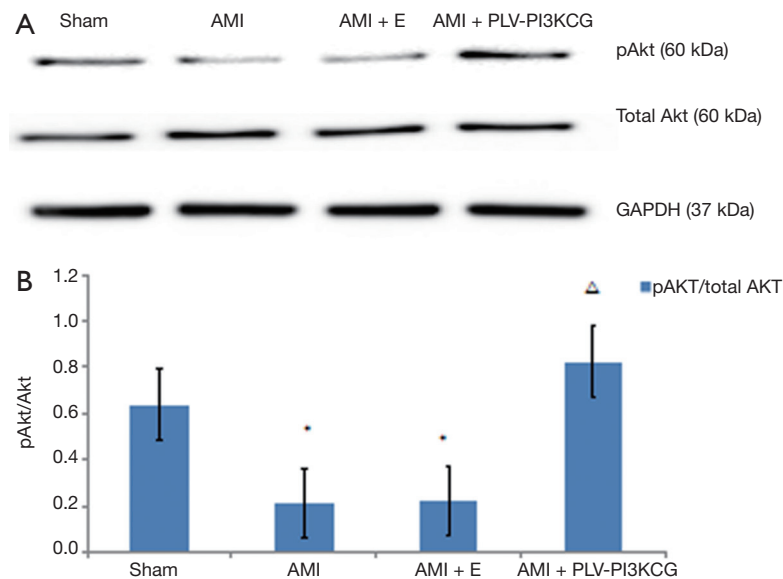
Figure 5 The PI3KCG, Bcl-2, Bax protein expressions among the four groups. (A) Compared with Sham group, in AMI group and AMI + E group, the PI3KCG, and Bcl-2 protein expressions were significantly decreased whereas Bax protein expression were significantly increased. Compared with AMI group and AMI + E group, in AMI + PLV-PI3KCG group, PI3KCG, and Bcl-2 protein expressions were significantly increased, whereas Bax protein expression were significantly decreased. (B) The PI3KCG/GAPDH ratio comparation among the four groups. Compared with Sham group, in AMI group and AMI + E group, the PI3KCG/GAPDH were significantly decreased. Compared with AMI group and AMI + E group, PI3KCG/GAPDH in AMI + PLV-PI3KCG group were significantly increased. (C) The Bcl-2/Bax ratio comparation among the four groups. Compared with Sham group, in AMI group and AMI + E group, the Bcl-2/Bax were significantly decreased. Compared with AMI group and AMI + E group, Bcl-2/Bax in AMI + PLV-PI3KCG group were significantly increased. *, compared with Sham group, $P<0.05$; $^{\triangle}$, compared with AMI group and AMI + E group, $P<0.05$. AMI, acute myocardial infarction.
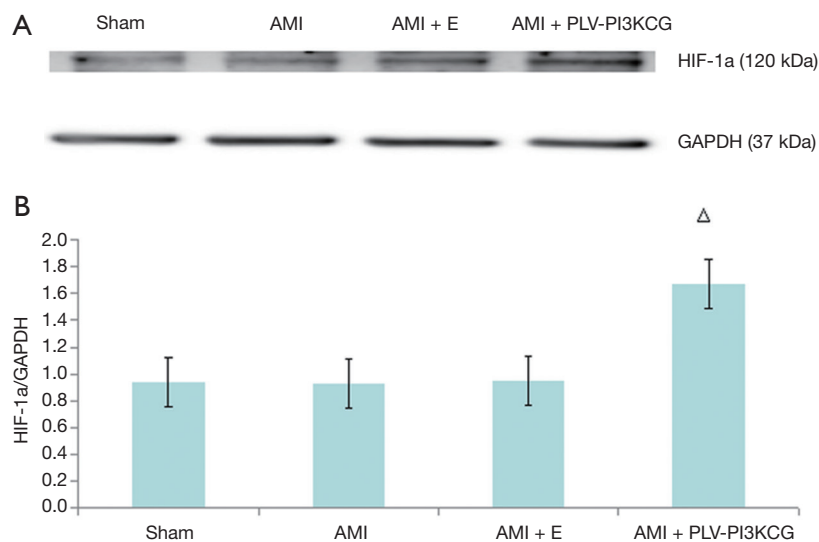
with AMI group and AMI + E group, heart function in AMI + PLV-PI3KCG group was significantly improved, myocardial tissue arranged neatly with less inflammatory cell infiltration. VEGF expression significantly increased; PI3KCG protein expressions and pAkt/Akt and Bcl-2/Bax ratios also increased. It is well known that VEGF is primarily expressed in vascular endothelial cells representing the angiogenesis extent. This result showed that *PI3KCG* gene might activate PI3K/Akt signaling pathway, which play a protective role in cardiomyocytes, help increase vascular endothelial cells significantly, promote the angiogenesis and increase myocardial oxygen supply. After the PI3K/Akt activation, Akt phosphorylation of various transcription factors can inhibit apoptosis Bax and cleaved Caspase 3 gene expression and enhance the expression of anti-apoptotic gene Bcl-2 by regulating these transcription factors, thereby

inhibiting apoptosis, promoting cell survival and decreasing the infracted size. The mechanism by which contractile parameters (LVEF% and FS%) increase by PI3KCG expression is associated with the reduced infracted size after the rPLV-PI3KCG injection.

Myocardial Apoptosis played an important role in the pathogenesis of AMI, so inhibition of apoptosis had become an important method for the treatment of AMI (13,14). PI3K/Akt was an important intracellular signal transduction pathway. Activation of Akt further activated or inhibited its downstream target proteins by phosphorylation, which further played a role in regulating cell proliferation, differentiation, glucose metabolism and migration (15-20). PI3K/Akt signaling pathway indirectly regulated calcium channels to influence myocardial contractility (21) and this pathway mediated cell growth and proliferation (22),

Figure 6 The pAkt, Akt protein expressions among the four groups. (A) The Akt protein expression was not significantly altered in the four groups. Compared with Sham group, the pAkt protein expression in AMI group and AMI + E group was significantly decreased. Compared with AMI group and AMI + E group, the pAkt protein expression in AMI + PLV-PI3KCG group was significantly increased. (B) The pAkt/Akt ratio comparation among the four groups. Compared to the Sham group, the AMI group and AMI + E groups had a significantly lower pAkt/Akt ratio. Compared with AMI group and AMI + E group, the AMI + PLV-PI3KCG group had a significantly higher pAkt/Akt ratio. It was suggested that the PI3KCG gene could play the protective role in the AMI injury process by activating the PI3K/Akt signal pathway and inhibiting apoptosis. *, compared with Sham group, $P<0.05$; △, compared with AMI group and AMI + E group, $P<0.05$. AMI, acute myocardial infarction.

Figure 7 The HIF-1α protein expressions among the four groups. (A) Compared with Sham group, the HIF-1α protein expression in AMI group and AMI + E group was not significantly altered. Compared with AMI group and AMI + E group, the HIF-1α protein in AMI + PLV-PI3KCG group was significantly increased. (B) The HIF-1α/GAPDH ratio comparation among the four groups. There was no significant difference between the Sham group, AMI group or AMI + E group. However, HIF-1α in the AMI + PLV-PI3KCG group had a significantly higher level than other three groups. △, compared with AMI group and AMI + E group, $P<0.05$. AMI, acute myocardial infarction.

protein synthesis (23), and apoptosis (24).

It has been shown that HIF-1α is the earliest expressed acute stage response factor associated with angiogenesis in the myocardial ischemia process (25). HIF-1α is only transiently activated and can induce VEGF expression and a series of hypoxia response and play the physiologic accommodation role (26). After myocardial ischemia for a few hours, it will begin to decline gradually till to the baseline level (27,28). In the current experiment, the HIF-1α protein was to be detected after the AMI operation for 10 days. Hence, the HIF-1α has already declined to the normal level in the AMI group and AMI + E group and no significant difference was observed in the AMI group, AMI + E group or Sham group. Researches have shown that activated PI3K/Akt signal pathway could increase HIF-1α expression (29,30). Therefore, the HIF-1α protein expression was significantly increased in the AMI + PLV-PI3KCG group in the present study. It was indicated that the higher HIF-1α expression level in the experiment group was associated with the PI3k/Akt signal pathway activation.

How does this relate to the underlying mechanism of enhanced Akt signaling? Pore *et al.* found that inhibition of PI3K in U87MG glioblastoma cells with LY294002 blunted the induction of HIF-1a protein and its targets VEGF and glut1 mRNA in response to hypoxia. They concluded that Akt1 activation can augment HIF-1a expression by increasing protein translation through a mammalian target of rapamycin-independent pathway (31). Sodhi *et al.* found that the HIF-1a oxygen-dependent degradation domain (ODD) does not contain an Akt phosphorylation consensus sequence. Their study suggested a mechanism whereby the PI3K/AKT signaling pathway may regulate HIF-1a protein stability through the inhibition of glycogen synthase kinase 3 (GSK-3) phosphorylation of the HIF-1a ODD. Thus, HIF-1a degradation was inhibited and synthesis was increased which promoted VEGF expression and angiogenesis (32). On the other hand, Ni *et al.* found that HIF-1α silencing could inhibit the activation of PI3K/Akt transduction signaling pathway in hepatoma cells (33). It suggested PI3K/Akt/HIF-1α/PI3K/Akt is a positive feedback loop.

Study limitations

Although it was already reported that PI3K (p110α) protects against MI-induced heart failure by Lin *et al.* (3), the AMI protection of PI3K (p110γ) has never been reported. However, there are some limitations in the current study.

In addition to the anti-apoptosis function of PI3KCG in the AMI process, autophagy might also participate in the ischemia myocardial injury process, the activation of PI3K/Akt on the cardiomyocytes anti-autophagy function need to be further explored.

Conclusions

The current work is the extension of the in vitro research published two years before which adds importantly to the knowledge how to diminish the ischemic myocardial damage (1). In summary, the *PI3KCG* gene successful expression could improve heart function after MI. This effect might be related to *PI3KCG* gene expression activating PI3K/Akt signaling pathway so as to activate HIF-1α signaling pathway for regulating apoptotic genes and anti-apoptotic genes; or it might be related to *PI3KCG* gene expression inhibiting autophagy that might cause damages, which played a protective effect against MI. This will lay the foundation for us to further explore the *PI3KCG* gene and PI3K/Akt signaling pathway in the future.

Acknowledgements

Footnote

Conflicts of Interest: The authors have no conflicts of interest to declare.

Ethical Statement: The current research was approved by the Ethics Committee of our institute (No. 2009-SR-033.1).

References

1. Li YY, Zhang H, Lu XZ. Lentiviral vector PLV-PI3KCG

gene transfer inhibits hypoxic cardiomyocytes apoptosis. Int J Clin Exp Med 2015;8:20208-17.

2. Vanhaesebroeck B, Guillermet-Guibert J, Graupera M, et al. The emerging mechanisms of isoform-specific PI3K signalling. Nat Rev Mol Cell Biol 2010;11:329-41.

3. Lin RC, Weeks KL, Gao XM, et al. PI3K(p110 alpha) protects against myocardial infarction-induced heart failure: identification of PI3K-regulated miRNA and mRNA. Arterioscler Thromb Vasc Biol 2010;30:724-32.

4. Liu S, Ai Q, Feng K, et al. The cardioprotective effect of dihydromyricetin prevents ischemia-reperfusion-induced apoptosis in vivo and in vitro via the PI3K/Akt and HIF-1α signaling pathways. Apoptosis 2016;21:1366-85.

5. Yang B, Yan P, Gong H, et al. TWEAK protects cardiomyocyte against apoptosis in a PI3K/AKT pathway dependent manner. Am J Transl Res 2016;8:3848-60.

6. Su Q, Li L, Zhao J, et al. Effects of nicorandil on PI3K/Akt signaling pathway and its anti-apoptotic mechanisms in coronary microembolization in rats. Oncotarget 2017;8:99347-58.

7. Li Y, Xia J, Jiang N, et al. Corin protects H2O2-induced apoptosis through PI3K/AKT and NF-κB pathway in cardiomyocytes. Biomed Pharmacother 2018;97:594-9.

8. Song CL, Liu B, Diao HY, et al. The protective effect of microRNA-320 on left ventricular remodeling after myocardial ischemia-reperfusion injury in the rat model. Int J Mol Sci 2014;15:17442-56.

9. Jiang X, Guo CX, Zeng XJ, et al. A soluble receptor for advanced glycation end-products inhibits myocardial apoptosis induced by ischemia/reperfusion via the JAK2/STAT3 pathway. Apoptosis 2015;20:1033-47.

10. Wang XL, Jiang SQ, Liu Y, et al. Curative effect of transplantion of cardiomyocyte-like cells on myocardial infarction rats. Chin J Cell Stem Cell (Electronic Edition) 2017;7:202-6.

11. Patel JR, Brewer GJ. Age-related differences in NFkappaB translocation and Bcl-2/Bax ratio caused by TNFalpha and Abeta42 promote survival in middle-age neurons and death in old neurons. Exp Neurol 2008;213:93-100.

12. Bakin AV, Tomlinson AK, Bhowmick NA, et al. Phosphatidylinositol 3-kinase function is required for transforming growth factor beta-mediated epithelial to mesenchymal transition and cell migration. J Biol Chem 2000;275:36803-10.

13. Paul A, Binsalamah ZM, Khan AA, et al. A nanobiohybrid complex of recombinant baculovirus and Tat/DNA nanoparticles for delivery of Ang-1 transgene in myocardial infarction therapy. Biomaterials 2011;32:8304-18.

14. Song JQ, Teng X, Cai Y, et al. Activation of Akt/GSK-3beta signaling pathway is involved in intermedin(1-53) protection against myocardial apoptosis induced by ischemia/reperfusion. Apoptosis 2009;14:1299-307.

15. Wallin JJ, Guan J, Prior WW, et al. GDC-0941, a novel class I selective PI3K inhibitor, enhances the efficacy of docetaxel in human breast cancer models by increasing cell death in vitro and in vivo. Clin Cancer Res 2012;18:3901-11.

16. Wallin JJ, Edgar KA, Guan J, et al. GDC-0980 is a novel class I PI3K/mTOR kinase inhibitor with robust activity in cancer models driven by the PI3K pathway. Mol Cancer Ther 2011;10:2426-36.

17. Chen K, Li G, Geng F, et al. Berberine reduces ischemia/reperfusion-induced myocardial apoptosis via activating AMPK and PI3K-Akt signaling in diabetic rats. Apoptosis 2014;19:946-57.

18. Salphati L, Wong H, Belvin M, et al. Pharmacokinetic-pharmacodynamic modeling of tumor growth inhibition and biomarker modulation by the novel phosphatidylinositol 3-kinase inhibitor GDC-0941. Drug Metab Dispos 2010;38:1436-42.

19. O'Brien C, Wallin JJ, Sampath D, et al. Predictive biomarkers of sensitivity to the phosphatidylinositol 3' kinase inhibitor GDC-0941 in breast cancer preclinical models. Clin Cancer Res 2010;16:3670-83.

20. Cheng G, Chunlei W, Pei W, et al. Simvastatin activates Akt/glycogen synthase kinase-3beta signal and inhibits caspase-3 activation after experimental subarachnoid hemorrhage. Vascul Pharmacol 2010;52:77-83.

21. Martelli AM, Nyakern M, Tabellini G, et al. Phosphoinositide 3-kinase/Akt signaling pathway and its therapeutic implications for human acute myeloid leukemia. Leukemia 2006;20:911-28.

22. Tabe Y, Jin L, Konopleva M, et al. Class IA PI3K inhibition inhibits cell growth and proliferation in mantle cell lymphoma. Acta Haematol 2014;131:59-69.

23. Pérez-Pérez A, Gambino Y, Maymo J, Goberna R, Fabiani F, Varone C, et al. MAPK and PI3K activities are required for leptin stimulation of protein synthesis in human trophoblastic cells. Biochem Biophys Res Commun 2010;396:956-60.

24. Vivanco I, Sawyers CL. The phosphatidylinositol 3-Kinase AKT pathway in human cancer. Nat Rev Cancer 2002;2:489-501.

25. Ivan M, Kaelin WG Jr. The von Hippel-Lindau tumor suppressor protein. Curr Opin Genet Dev 2001;11:27-34.

26. Lee JW, Bae SH, Jeong JW, et al. Hypoxia-inducible factor (HIF-1)alpha: its protein stability and biological functions. Exp Mol Med 2004;36:1-12.
27. Jiang C, Lu H, Vincent KA, et al. Gene expression profiles in human cardiac cells subjected to hypoxia or expressing a hybrid form of HIF-1 alpha. Physiol Genomics 2002;8:23-32.
28. Poellinger L, Johnson RS. HIF-1 and hypoxic response: the plot thickens. Curr Opin Genet Dev 2004;14:81-5.
29. Kitajima Y, Miyazaki K. The critical impact of HIF-1a on gastric cancer biology. Cancers (Basel) 2013;5:15-26.
30. Movafagh S, Crook S, Vo K. Regulation of hypoxia-inducible factor-1a by reactive oxygen species: new developments in an old debate. J Cell Biochem

2015;116:696-703.
31. Pore N, Jiang Z, Shu HK, et al. Akt1 activation can augment hypoxia-inducible factor-1alpha expression by increasing protein translation through a mammalian target of rapamycin-independent pathway. Mol Cancer Res 2006;4:471-9.
32. Sodhi A, Montaner S, Miyazaki H, et al. MAPK and Akt act cooperatively but independently on hypoxia inducible factor-1alpha in rasV12 upregulation of VEGF. Biochem Biophys Res Commun 2001;287:292-300.
33. Ni JY, Wu YD, Xu LF, et al. Effects of HIF-1α silencing on the PI3K/AKT transduction signaling pathway in hepatoma cells. Chinese Journal of Cancer Prevention and Treatment 2014;21:356-9.
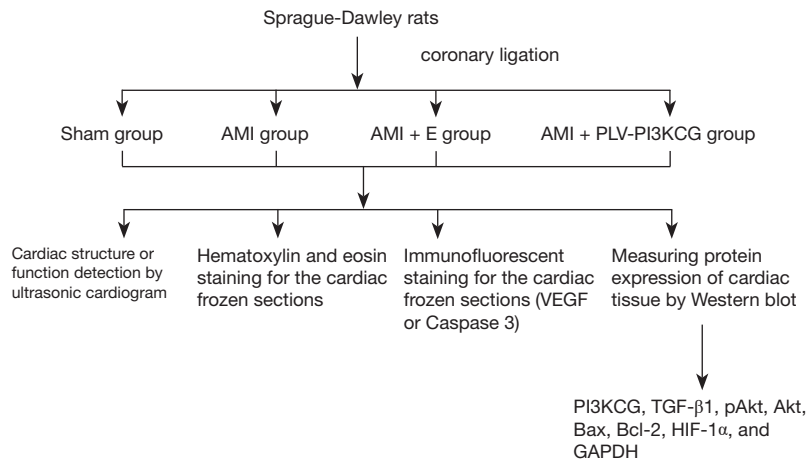
Figure S1 The graphic demonstration of the study design.
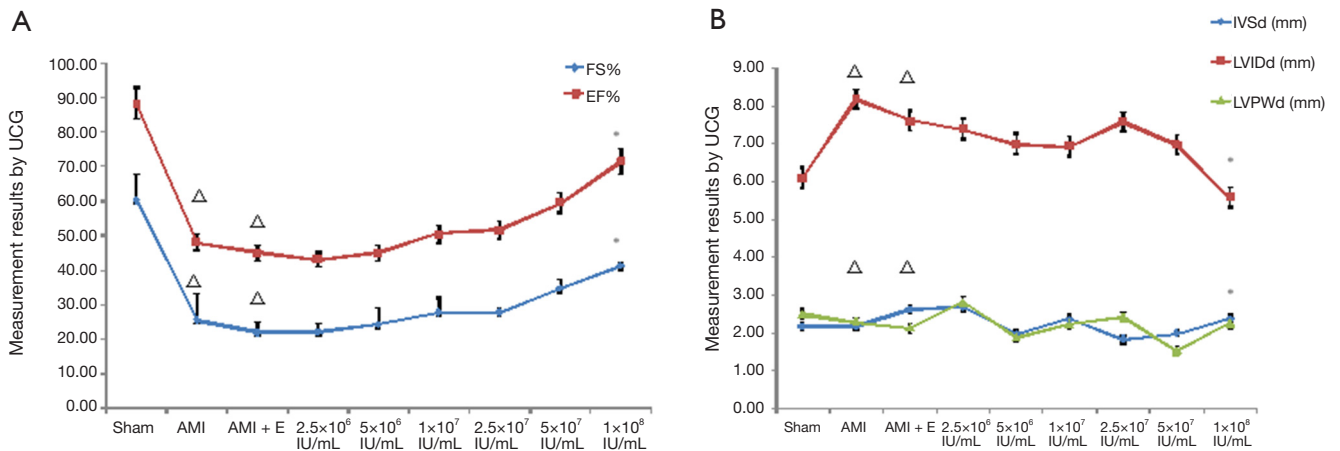
Figure S2 Effects of *rPLV-PI3KCG* different titer on cardiac function or structure changes detected by UCG. (A) The Effects of rPLV-PI3KCG different titer on LVEF% (EF%) and FS% changes results detected by UCG. Compared with AMI group, AMI + E group and other different titer groups in the 1×10^8 IU/mL group, the LVEF%, FS% were significantly increased (P<0.05). Compared with Sham group, in the AMI group, AMI + E group and other different titer groups, the LVEF%, FS% were significantly decreased (P<0.05). (B) The Effects of rPLV-PI3KCG different titer on IVSd, LVEDd (LVIDd) and LVPWd changes results detected by UCG. Compared with AMI group, AMI + E group and other different titer groups in the 1×10^8 IU/mL group, LVEDd was significantly decreased (P<0.05). Compared with Sham group, in the AMI group, AMI + E group and other different titer groups, LVEDd was significantly increased (P<0.05). *, compared with AMI group, AMI + E group, P<0.05; ᐃ, compared with Sham group, P<0.05. AMI, acute myocardial infarction; IVSd, interventricular septal thickness at diastole; LVEDd, left ventricular end diastolic diameter; LVPWd, left ventricular posterior wall diastolic diameter; UCG, ultrasonic cardiogram.